

Application of a Virtual Reactivity Feedback Control Loop in Non-Nuclear Testing of a Fast Spectrum Reactor

Shannon M. Bragg Sitton¹ and Matthew Forsbacka²

¹NASA Marshall Space Flight Center, Huntsville, Al, 35812 Tel: (256) 544-6272, Shannon.Bragg-Sitton@msfc.nasa.gov;

²NASA Headquarters, 300 E St. S, Washington, DC 20465

Abstract – For a compact, fast-spectrum reactor, reactivity feedback is dominated by core deformation at elevated temperature. Given the use of accurate deformation measurement techniques, it is possible to simulate nuclear feedback in non-nuclear electrically heated reactor tests. Implementation of simulated reactivity feedback in response to measured deflection is being tested at the NASA Marshall Space Flight Center Early Flight Fission Test Facility (EFF-TF). During tests of the SAFE-100 reactor prototype, core deflection was monitored using a high resolution camera. "Virtual" reactivity feedback was accomplished by applying the results of Monte Carlo calculations (MCNPX) to core deflection measurements; the computational analysis was used to establish the reactivity worth of various core deformations. The power delivered to the SAFE-100 prototype was then adjusted accordingly via kinetics calculations. The work presented in this paper will demonstrate virtual reactivity feedback as core power was increased from 1 kW_e to 10 kW_e, held approximately constant at 10 kW_e, and then allowed to decrease based on the negative thermal reactivity coefficient.

I. INTRODUCTION

Development of a nuclear reactor for space application will require a significant amount of testing prior to deployment of a flight unit. High confidence in postulated fission system thermal-hydraulic performance can be obtained through a series of non-nuclear tests, with the heat from nuclear fission simulated using electric resistance heaters. Because of the close coupling of reactor dynamics and thermally-driven core dimensional changes during operation, electrically heated core simulations can add additional insight into reactor performance during startup and power maneuvering. Through demonstration of system concepts in relevant environments, non-nuclear tests have proven to be a highly effective method to identify and resolve integration issues, from both cost and performance standpoints.¹⁻⁴

A set of non-nuclear experiments was conducted on the "Safe Affordable Fission Engine" ('SAFE') heat pipe cooled reactor (HPR) design.²⁻⁴ The 'SAFE'-HPR is a compact, fast-spectrum reactor designed to use highly enriched UN fuel. In this design, passive heat extraction from the reactor core is accomplished by in-core liquid metal heat pipes. The condenser section of the heat pipes is then coupled to two or three heat exchangers. Multiple heat exchangers are proposed to mitigate the risk of a single point failure.⁵

Experiments were performed on the 'SAFE'-100 prototype, designed to provide 100 kW_e power. The 'SAFE'-100 HPR would be equipped with 61 modules, each containing three fuel tubes and one heat pipe. In the prototype, a total of 183 graphite resistance heaters were used to simulate the heat of nuclear fission. The prototype discussed in the present application had no mechanism for heat removal from the core; hollow stainless steel tubes were used to represent the heat pipe in each module. As a result, this prototype was used to simulate the operation of a fission system in the absence of cooling; this condition is similar to the operation of an HPR during the start-up period prior to complete thaw of the heat pipe working fluid and initialization of the heat exchangers. Deflection tests were performed on a 316 stainless steel (SS316) core, which was manufactured according to the 'SAFE'-100 core fabrication drawings. The 'SAFE'-100 is a scaled-down version of higher power HPR systems that could be applied in nuclear electric propulsion (NEP) systems.⁵ Due to relatively high operating temperatures, prototypical space nuclear reactors for electric propulsion applications would likely use refractory metals in place of the stainless steel used to construct the 'SAFE' prototype.

The work presented in this paper includes measurement of core deformation due to material thermal expansion and implementation of a virtual reactivity feedback control loop.

II. CORE THERMAL EXPANSION AND VIRTUAL REACTIVITY FEEDBACK

For compact, fast spectrum reactors, reactivity feedback is dominated by core deformation. As the core temperature increases, the reactor materials expand, resulting in a larger geometry and reduced material densities. The effects of the geometric and material density changes in the reactor core can be simulated experimentally by coupling electrically heated reactor tests with neutronic analyses that establish the reactivity worth of various core deformations. Deformation from the original geometry can be measured, the reactivity change can be assessed from Monte Carlo calculations,⁶ and the corresponding core power as a function of time can then be computed via solution of the point kinetics equations. Rapid iteration of this control loop can provide a mechanism for the power applied to an electrically heated core to match the calculated neutronic response of the corresponding nuclear system.

II.A. Set-up of Test Hardware

Core deflection was measured using high resolution photography. Imagery from a 6.3 mega-pixel high resolution camera, composed of a charged couple device (CCD) and a camera lens, was used to assess core deflection as a function of temperature by scanning multiple cross sections along the axial dimension of the core. The radial core size was determined from the number of pixels across each profile. Comparison of a time series of core snapshots referenced to room temperature snapshots provided the core deflection as a function of time. Prior to application in the virtual reactivity feedback loop, imaging results were validated by comparison to mechanical caliper measurements up to ~450° C.

Testing was performed inside a nine foot diameter vacuum chamber, with support hardware located just outside the chamber. The reactor core prototype was located on an immobile stand inside the chamber, and the CCD imaging system had a clear view of the core through a fused silica viewing port, as shown in Fig. 1.

The reactor core prototype was equipped with axially shaped graphite heater elements to simulate nuclear fuel elements, providing an axial power profile predicted to be equivalent to that of an operating nuclear reactor. Each heater was fitted with three alumina (Al_2O_3) insulator rings, located at each end and at the center, to prevent the heater from shorting to the fuel tube. The 'fuel tube' refers to the stainless steel tube that the heater slides into, simulating the clad that would surround a nuclear fuel element.

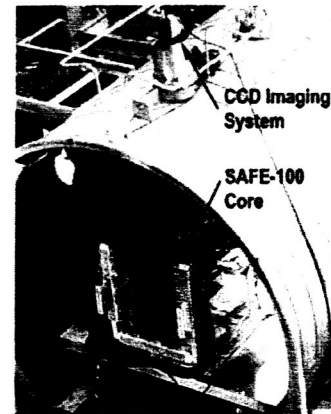


FIGURE 1. 'SAFE'-100 Test Hardware Setup

The virtual reactivity feedback experiment called for real-time monitoring of the variations in core deflection, determination of the corresponding reactivity worth of measured deflections from neutronic simulations performed off-line, and calculation of a new solution to the point kinetics equations to appropriately adjust the predicted reactor power. Communication between the control system and power supplies was provided by an Ethernet network, resulting in a response time on the order of 100 ms, and the control system utilized National Instruments LabView VI's and compact field points units.

The reactor core prototype was configured to operate using nine control zones, accomplished by connecting the 183 heaters in nine concentric heater rings. Application of different power levels to each control zone provided the capability to match the predicted radial power profile for the 100 kW, HPR.

To monitor temperature, the reactor core prototype was equipped with 32 internal thermocouples distributed evenly throughout the core, positioned in the hollow stainless steel tubes representing the core heat pipes. The thermocouples were pushed into the blank modules from the end opposite the power feed-through to the heaters, such that the probe ends were located near the axial center of the 55 cm long core. The probes were not bonded or attached to the interior surface of the modules, leaving the thermocouples to rest at the center location. The precise location of the probe tips was not verified, and some probes may have been in contact with the module tube wall. An additional series of thermocouples was spot-welded to the perimeter of the core to provide surface temperature data. Placement of internal and perimeter thermocouples is shown in Fig. 2.

Based on previous test experience, the core support structure was modified prior to implementing the virtual reactivity feedback experiment. To minimize jerky motion during core expansion, the reactor core prototype was fixed to allow radial expansion in only one dimension. One side of the core was fixed to the support frame while

the other side was allowed to move freely. On the "free" side, the core supports rested on rollers to allow free radial expansion, as shown in Fig. 2. Only one of the fixed points was bolted firmly to the frame, allowing for axial expansion.

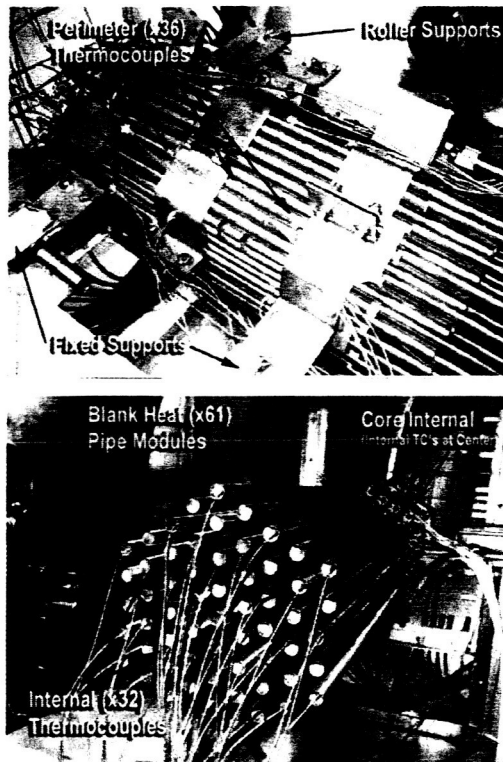


FIGURE 2. Identification of 'SAFE'-100 Core Prototype Support Structure and Thermocouple Placement.

II.B. Deflection Measurements: CCD Imaging System

The CCD imaging system was configured to measure the radial core width at several axial locations; the selected locations are shown as D1, D2, and D3 in Fig. 3. For the selected camera field of view settings, each pixel had a width of 0.09 mm (in the radial direction). At each location, an averaging "box" (containing several edge pixels) rather than a sampling line (containing only a single edge pixel), was incorporated to improve the robustness of the imaging system. Validation of the CCD imaging system and consideration of other measurement options are discussed by Stanojev.⁷

The core width was measured at room temperature along three CCD sampling lines using a caliper. These measurements were used to calibrate the CCD measurement in the LabView control program. The camera field of view (FOV) settings provided a CCD pixel size of approximately 0.09 mm.

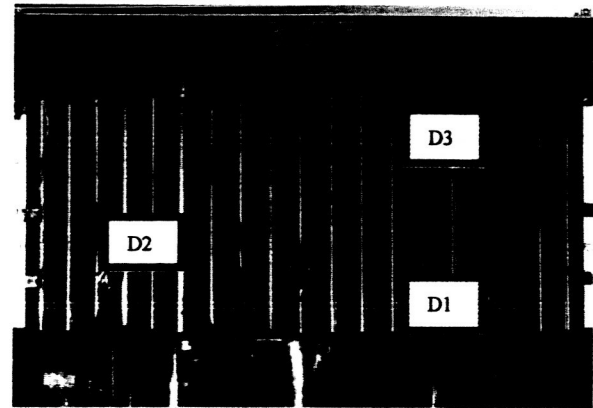


FIGURE 3. Screen Shot Taken During Test Identifying Three Axial Locations for Core Width Measurement.

For a measurement taken along a single pixel width at a single time point, the CCD resolution corresponds to one pixel, or 0.09 mm. However, spatial and temporal averaging can be used to improve the measurement resolution. Incorporating a spatial averaging box containing multiple edge pixels removes bias that could exist due to the selection of the precise location of the cross section. In addition, a spatial average can account for small deviations in the straightness of the core or a small amount of twist in the core positioning. Twist could result in a slightly diagonal cross section in lieu of a cross section that is precisely perpendicular to both core edges.

To determine the resolution of the CCD imaging system with spatial averaging over a 30 pixel (2.7 mm) slice thickness, data were acquired for approximately one hour with the core at room temperature and at vacuum conditions ($\sim 10^{-4}$ Torr). A noise analysis was performed on the resultant data, taken at one second intervals. For the centermost profile (identified as "D2" in Fig. 3), the mean pixel width at room temperature was 2894.147 pixels with a corresponding standard deviation of 0.0736 pixels. This corresponds to a measurement resolution of 0.0736 pixels * 0.09 mm/pixel, or 0.0068 mm.

To further improve the measurement resolution, a temporal average of the CCD data was implemented. A five point moving average was constructed, such that the reported value at a given time point corresponded to the average of the values for the previous five seconds (data were still reported every second). Given spatial and temporal averaging, the mean pixel width of the core was 2894.149 pixels, only 0.002 pixels larger than the mean width in the one second data, with a standard deviation of 0.0379 pixels. This corresponds to a measurement resolution of 0.0379 pixels * 0.09 mm/pixel, or 0.0035 mm.

Due to the improved measurement resolution, deflection measurements for the virtual reactivity feedback

loop applied a 30 pixel spatial average and a 5 second temporal average.

II.C. Thermal Expansion and Core Neutronics

The reactivity worth of various core deflections was determined from a series of MCNPX calculations⁶ that were performed to develop an empirical relationship for reactivity as a function of gross core deflection.

As reactor core temperature increases, the materials in the core begin to deform. Although the deformation is relatively small (a few mm), it can have a significant impact on the core reactivity as a result of the dominance of leakage in compact fast reactors.⁸ Because the predominant material in the reactor core prototype was stainless steel (SS-316), it was assumed that core deflection would be dominated by the thermal expansion of SS-316. The coefficient of thermal expansion (CTE) for SS-316, as a function of temperature, has been determined from a number of experimental measurements.⁹⁻¹⁰ A least squares fit to this data yields:

$$CTE(T) = -1.76 \cdot 10^{-11} T^4 + 5.71 \cdot 10^{-8} T^3 - 7.01 \cdot 10^{-5} T^2 + 4.27 \cdot 10^{-2} T + 6.99, \quad (1)$$

where T is the material temperature in degrees Kelvin and CTE is in 10^{-6} mm/mm/K.

To simulate core deformation in MCNPX calculations, the entire core was uniformly expanded both radially and axially based on the thermal expansion characteristics of SS316 at a given temperature, making the corresponding adjustment to the material density in the MCNPX input file. As the core materials were expanded in the model, the material density was decreased and the gaps in the core (e.g., between fuel and clad) were narrowed. No axial bowing effects were modeled, nor was Doppler broadening applied to the material cross sections at elevated core temperatures. Calculations performed by J. Durkee at Los Alamos National Laboratory on a larger reactor design (500 kW_t) demonstrated that Doppler broadened cross sections would not be expected to significantly impact the core reactivity. Calculations indicated that the core multiplication factor increased less than 0.05% when Doppler broadened cross sections were included.¹¹

All neutronic calculations were performed using MCNPX with the 'SAFE'-400 design model. Conceptually, the heat pipe reactor was designed to be scalable, maintaining similar geometric configuration and component sizes.⁵ For example, the 'SAFE'-100 and 'SAFE'-400 designs both maintained a core flat-to-flat size of 26 cm (distance between opposing sides of the hexagonal core) and a fueled height of 50 cm, yielding expected similarity in neutron leakage properties.¹² Therefore, it was assumed that the effect of elevated

temperature on core reactivity would have a similar trend in the 'SAFE'-100 and 'SAFE'-400 designs. To more accurately describe the prototype, all the refractory metal structure in the MCNPX model was replaced by SS-316 in the simulation. The experimental application presented here demonstrates the capability to couple non-nuclear testing with nuclear simulations to better replicate the response of an operating reactor to geometric and material changes. Future applications of this testing methodology will attempt to more precisely model the test article in the nuclear simulations.

Prototypical space nuclear reactor designs for electric propulsion applications will likely use refractory metals (e.g., Niobium - Zirconium Alloys) and will potentially use liner materials such as Rhenium. The current state of cross-section uncertainties for the elements Re and Nb will necessitate further studies to factor in the systematic reactivity impact due to these elements in NEP systems.

In the present experiment, criticality calculations were performed using MCNPX for the stainless steel 'SAFE'-400 core with the control drums at various positions. Calculations assumed that all six control drums moved simultaneously and symmetrically. Fig. 4 shows the reactivity (ρ) as a function of core deformation for control drums rotated 120° and 90° from the full-in position. The total core deformation is given by $CTE(T) \cdot L_0$, where L_0 is the original core diameter at room temperature. The center curve (control drums at 106°) was constructed by linear interpolation from the 120° and 90° results to illustrate the effect of increasing temperature on an initially critical reactor core ($\rho = 0$). Error bars correspond to one standard deviation and were calculated from the statistical error in the MCNPX calculation of the multiplication factor k, where $\rho = (k-1)/k$. Calculations assumed that the entire core was at a uniform temperature, generating uniform core deformation. The corresponding core temperatures are indicated on the vertical profile lines superimposed on the reactivity plot.

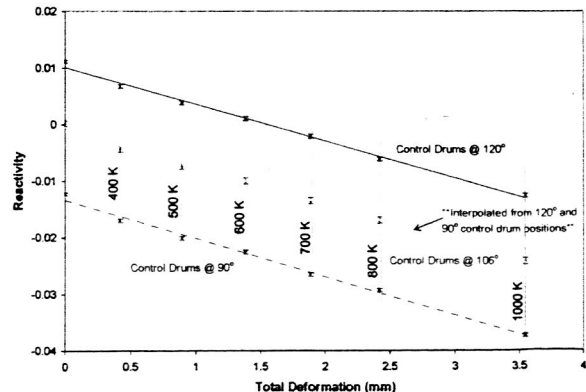


FIGURE 4. 'SAFE'-400 Reactivity (SS-316 Core) as a Function of Core Deformation.

A sensitivity analysis was performed at 400 K, 800 K, and 1000 K to determine the potential error associated with expansion of the entire core based on the properties of stainless steel. The most sensitive component in the reactor core is the nuclear fuel; variations in the fuel geometry can significantly impact the core neutronics. Expansion of the uranium nitride (UN) fuel was considered for three scenarios at 400 K: no UN expansion, expansion based on the CTE for UN, and expansion based on the CTE for SS-316. The latter two cases were also considered at the higher temperatures of 800 K and 1000 K. The CTE for UN at 900 K (627° C) is $8.5 \times 10^{-6} / ^\circ\text{K}$.¹² Because this was the only available data point, it was applied for UN expansion at all temperatures.

Results of the sensitivity analysis provided in Table 1 reveal no significant differences in the calculated reactivity at the tested temperatures. These results suggest that no significant error was introduced by assuming that core deformation was dominated by the properties of stainless steel.

The results provided in Fig. 4 indicate that core deformation significantly affects reactivity for a stainless steel reactor core. A refractory metal core matrix, on the other hand, would experience significantly reduced deflection at the same temperatures, as shown in Fig. 5. The corresponding reduction in the negative reactivity feedback is shown in Fig. 6 for a refractory metal core.

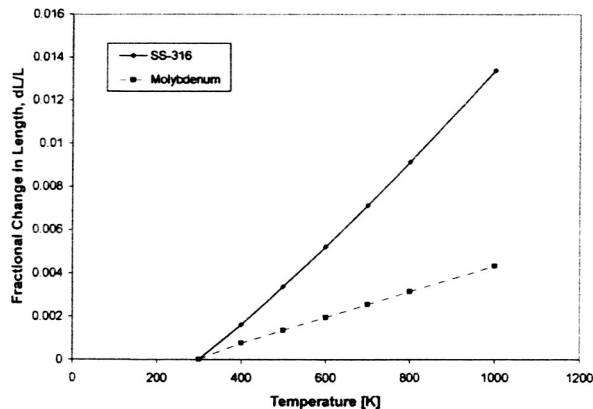


FIGURE 5. Thermal Expansion of Stainless Steel 316 and Molybdenum Metal as a Function of Temperature.

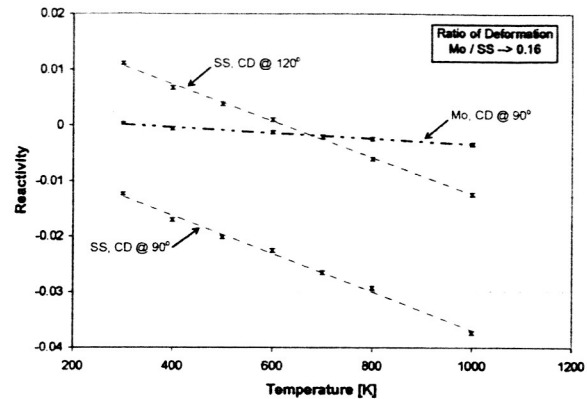


FIGURE 6. 'SAFE'-400 Reactivity as a Function of Core Temperature.

II.D. Radial Power Profile

For the virtual reactivity feedback loop, nine control zones were used to simulate the appropriate radial power profile of an operating reactor. Each control zone in the reactor core prototype was equipped with its own power supply, each capable of providing 15 kW of power. Neutronic calculations were performed using MCNPX for the 'SAFE'-400 design; these results were used to determine the appropriate radial power profile for the 'SAFE'-100 tests. The nine control zones applied in the deflection tests are shown in Fig. 7. Table 2 provides the zone identifiers and the corresponding fraction of the total power applied to each control zone. The innermost ring corresponds to control zone 1; the outer ring is control zone 9.

II.E. Reactor Model: Point Kinetics

Given the total "virtual" reactivity in the simulated reactor at a given time, the power delivered to the reactor core prototype was determined by solution of the point kinetics equations (PKE) for the predicted reactor power, $P(t)$. The PKE applied in the feedback loop were solved in the absence of an external source and for one group of delayed neutrons. Written in terms of power, the system of differential equations is given by Eqns. (2).

Condition	Temperature [K]		
	400	800	1000
no UN expansion	1.00774 ± 0.00033	-----	-----
UN expansion with CTE for UN	1.00675 ± 0.00033	0.99546 ± 0.00032	0.98827 ± 0.00032
UN expansion with CTE for SS	1.00674 ± 0.00032	0.99437 ± 0.00034	0.98814 ± 0.00034
Percent Difference	0.001 - 0.1 %	0.1 %	0.01 %

TABLE 1. Calculated Effective Multiplication Factor at the Indicated Temperature and Conditions.

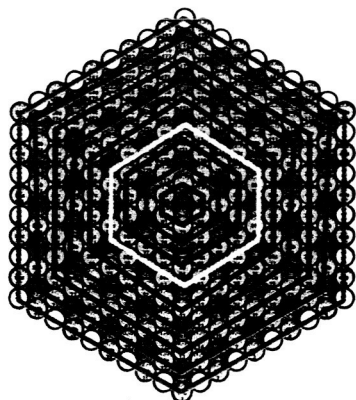


FIGURE 7. 'SAFE'-100 Control Zone Map.

$$\frac{dP}{dt} = \frac{(\rho - \beta)}{\Lambda} P + \lambda C \quad (2a)$$

$$\frac{dC}{dt} = \frac{\beta}{\Lambda} P - \lambda C \quad (2b)$$

The total reactivity is given by the sum of the drum reactivity at the specified control drum position and the reactivity worth of the core deflection,

$$\rho_{total} = \rho_{drum} + \rho_{dL} \quad (3)$$

The drum reactivity for the stainless steel 'SAFE'-400 reactor core was determined by MCNPX calculation with the control drums rotated 60°, 90°, and 120° from the full-in position. A simple empirical relationship $\rho(\theta)$ was fit to the calculated data points using a least-squares fitting algorithm. Because only a small range of angular motion was anticipated for the control loop, a simple second order polynomial was selected for the relationship, yielding:

$$\rho_{drum} = \rho(\theta) = -3.85 \cdot 10^{-6} \theta^2 + 1.59 \cdot 10^{-3} \theta - 0.124, \quad (4)$$

where the angle θ is given in degrees. Fig. 4 indicates that the reactivity worth of the core deformation maintained a linear relationship (with approximately the same slope) regardless of the initial control drum configuration. Therefore, an expression for ρ_{dL} was determined by a linear fit for an initially critical reactor ($\theta \sim 106.427^\circ$).

$$\rho_{dL} = \rho(dL) = -1.864 \cdot \frac{dL}{L_o}, \quad (5)$$

where L_o is the initial core diameter at room temperature and dL is the measured deflection from the start of the experiment.

Control Zone	Color	Power Supply	Fraction of Power
1	Navy	F1	0.134
2	Aqua	G1	0.133
3	Brown	G2	0.129
4	Yellow	G3	0.123
5	Purple	G4	0.117
6	Orange	H1	0.107
7	Black	H2	0.098
8	Green	H3	0.086
9	Pink	H4	0.072

TABLE 2. Fractional Power Levels for Each Control Zone.

The reactor power, $P(t)$, and the delayed neutron concentration, $C(t)$, were solved in real time given variations in the core reactivity, ρ_{total} . The solution for $P(t)$ was used to determine the power applied to the nine control zones. Although the precursors could not be simulated in the electrically heated core, the solution for $C(t)$ was used to find new initial conditions at each point the control loop was iterated.

III. TEST PROCEDURE

The virtual reactivity test procedure required a physical measurement of the core width to provide a zero-point for the CCD imager, locking the initial core dimensions in the data acquisition code. Using mechanical calipers and real-time image guidance, initial core measurements were taken at each of the three cross sections identified in Fig. 3 to calibrate the system. Growth was tracked along all three selected cross sections, but the LabView control program only assessed growth at the centermost cross section, D2, to modify the calculated reactivity and to implement control loop cycles.

After initial calibration measurements were completed, the vacuum chamber was evacuated to approximately 10^{-4} Torr. The bank of tubes used to construct the reactor core prototype was held together by three steel clamps along the axial length of the core without any interstitial material (e.g., braze) between core modules. To improve core coupling, the vacuum chamber was back-filled with approximately 50 Torr of argon gas to provide a medium for heat conduction between the individual stainless steel tubes. Compared to a vacuum environment, inert gas better simulated the coupling in an actual reactor core in which modules would be brazed together or inserted into a monolithic block.

The initial caliper measurements were input into the CCD data acquisition program to calibrate the CCD measurement and to lock the initial core size to the reference image at the current environmental conditions.

The core was then initialized to a low initial power (P_0) of 1 kW_t. The initial precursor concentration (C_0) was found from the steady state solution of the PKE at P_0 .

With the power initialized to 1 kW_t, the average core temperature, calculated from an average of thermocouple measurements across the core radius, was allowed to increase to 150–200° C prior to implementation of the reactivity feedback loop. Due to the power peaking in the central region of the core and the lack of any mechanism for heat removal, the inner region of the core was at significantly higher temperature than the outer regions. As a result, a relatively high average core temperature was required to increase temperatures at the core periphery before measurable deflection was detected by the CCD imaging system.

When initializing the core at low power, it was assumed that the control drums in the corresponding nuclear system were positioned such that the reactor was critical. Hence, the “virtual” control drums in the electrically heated core were also set to a position such that $\rho_{\text{drum}} = 0$ at P_0 . For the stainless steel version of the 'SAFE'-400 core, criticality at 300 K (room temperature) corresponded to a drum position of 106.427° C.

After reaching the desired initial power and temperature, the control loop was initiated. The theoretical control drums were perturbed to insert positive reactivity and to increase core power. The corresponding $P(t)$ was found by solution of the PKE for the given ρ_{drum} , and the reactor power was allowed to increase along this curve until a deflection greater than a pre-set value Δ_{set} was measured. The measured deflection (Δ) is the deflection measured since the previous calculation of $P(t)$, such that $\Delta = dL_{\text{total}} - dL_{\text{previous}}$. The Δ_{set} value was set with respect to the measurement resolution of the CCD deflection measurement. With spatial (30 pixel) and temporal (5 second) averaging implemented, the CCD resolution was 0.0035 mm. In this application, an appropriate Δ_{set} was 0.01 mm, approximately three times the measurement resolution. This value was set just prior to implementation of the control loop, but initial tests also allowed adjustments to Δ_{set} during test to permit the user to get a better feel for the system response prior to implementation of fully automated control.

When the desired core deflection was measured, the solutions to the PKE were recalculated to better simulate the response of a nuclear system to the measured change in core geometry. The deflection used to calculate the new initial conditions (P_0 , C_0) from the PKE was given by $dL_{\text{calc}} = dL_{\text{previous}} + \frac{1}{2} \Delta$. Because an operating nuclear reactor would not have precisely followed the previous $P(t)$ that was applied to the power controllers, but instead would have been continuously updated based on the real-time geometric changes in the core, calculation of P_0 , C_0 using half of the measured deflection (Δ) allowed a small amount

of adjustment to the electrically heated system to better match the power and precursor concentration in the corresponding nuclear system. The recalculated initial conditions were then used to solve the PKE for the next iteration of the control loop.

To solve for the new $P(t)$ and $C(t)$, the total measured deflection from time zero (dL_{total}) was applied. Prior to calculation of the new $P(t)$, the current value of the total reactivity was assessed. Given a positive reactivity, the control loop automatically recalculated the power $P(t)$ and continued operating as in the previous loop iteration. However, if the current measured deflection introduced sufficient negative reactivity to cause the total reactivity to become negative or zero, additional positive reactivity was inserted by perturbation of the control drums. This additional perturbation was required to continue to either increase power or to maintain the current power level. To simulate natural reactor shut down as a function of negative feedback effects, the “virtual” control drums were left in a constant position. Without heat extraction from the core, the core temperature continued to increase, resulting in further deformation, causing the controller to decrease power as a result of the negative reactivity feedback.

IV. RESULTS

The virtual reactivity feedback test was operated several times in “manual” mode to work out any programming issues in the LabView control code written specifically for this application. In the initial tests, the reactor power transient calculated by LabView for a given virtual control drum position and measured deformation were verified off-line by direct solution of the reactor point kinetics equations. When operated manually, the controller measured core deflection automatically, but then required user intervention to implement the control loop when the desired deflection was reached. In addition, manual adjustments to the virtual control drum positions were required throughout the test. Future versions of the controller will automatically recalculate $P(t)$ and $C(t)$ after reaching the desired deflection, automatically adjusting the virtual control drum position to achieve and maintain the desired goal power level.

IV.A. Initialization of Core Power

In all tests, the reactor core was initialized by applying approximately 1 kW_t to the full core. This was accomplished by setting the current for each control zone to a maximum of 6.5 A, allowing the power controller to determine the appropriate current in each zone to obtain the desired radial power profile. Upon application of power to the core, the measured core size along all three sampled cross sections initially decreased, reporting a negative

deflection after approximately 100–200 seconds. This behavior was observed in all deflection tests. As the average core temperature began to increase, the core size reached a minimum before beginning to increase once again. In the results presented here, the core reached its original size at an average temperature of approximately 180° C. This behavior is evident in Fig. 8, which corresponds to the initial 9000 seconds of operation. A decline in the measured core size was readily evident, with a subsequent rise over the remaining period. In this test, the control loop was initiated at approximately 7900 seconds, when the center core cross section, D2, indicated that the core had returned to its original size.

Possible sources of this unexpected decline in core size could be electrical noise, effects of elevated environmental temperature, or “reordering” of the core modules as a result initial stresses placed on the core. If electrical noise was responsible for the behavior, the decline in core size would be expected to immediately follow initialization of the power. However, a focused analysis indicated that the decrease in core size was not immediate, but began to occur after approximately 200 seconds, eliminating the possibility that electrical interference generated an artificial decrease in the measured core size.

Elevated environmental temperature could also effect the camera operation. However, the decrement in core size occurred before any significant heating of the core module was measured (average core temperature ~ 50° C), suggesting that temperature effects were not a significant component of the unexpected behavior.

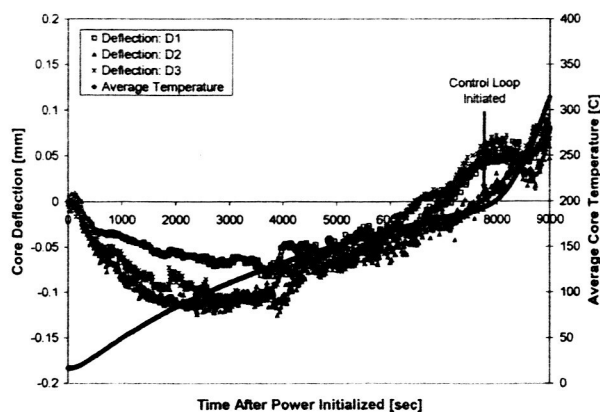


FIGURE 8. Measured Core Deflection During Initial Core Heat Up.

Pre-stressing of the core by the core clamping structure was the most likely source of the initial decrement in the measured core size. The three steel clamps that held the core modules together (Fig. 2) were tightened snugly to the core, applying initial compression stress. As the core heated up, the temperature of the center

modules increased much more quickly than the temperature of the modules on the periphery, causing the interior modules to deform earlier than the remainder of the core. Because the core elements were not precisely straight or round, early deformation of the interior core elements caused the remainder of the elements to shift slightly given the assistance of the clamping stresses applied at the periphery. At the point when the internal expansion stresses exceeded the initial clamping stresses and the temperature of the clamps themselves began to rise, the core diameter could physically increase once again, explaining the peculiar behavior observed by the CCD imaging system.

IV.B. Feedback Control

The objective of the virtual reactivity feedback test was to increase core thermal power from an initial power level of approximately 1 kW_t to approximately 10 kW_t, to hold the goal power level at steady state, and to allow natural shutdown of the simulated reactor based on negative reactivity inserted by core deformation. Because there was no mechanism for heat removal in the 'SAFE'-100 prototype, the reactor temperature continued to increase when the core was held at a constant (or decreasing) power level. Therefore, the goal power level of 10 kW_t could be held for only a limited time before the temperatures at the center of the reactor core approached levels that could cause damage to system components.

Fig. 9 shows the calculated and applied thermal power and the corresponding virtual control drum positions for the full duration of the test. The deflection measurement at each of the three monitored core profiles returned to zero at an average core temperature of 185° C, at which point the control loop was initiated with a drum perturbation of 0.563° (106.427° to 107°). In this application, the initial core power was 1.4 kW_t when the control loop was implemented. After each measured deflection of 0.02 mm ($\Delta_{set} = 0.02$ mm), the solutions to the PKE were recalculated and the core power, P(t), was adjusted accordingly. Early in the operation, each recalculation of P(t) and C(t) (each control loop iteration) resulted in a slight bump in the calculated and applied power. This behavior resulted from re-calculation of the new initial conditions using only half of the measured deflection from the previous iteration. As the rate of change of the power decreased, readjustment of the initial conditions for the next loop iteration was less evident. A smaller value of Δ_{set} may be used to minimize the affect of readjusting the PKE, but limitations in the measurement resolution of the CCD imaging system prevent reduction of Δ_{set} much below 0.01–0.02 mm.

The measured core deflection lagged the increase in the average core temperature. This delayed response resulted from the radial temperature profile. The increase

in the average temperature was primarily driven by the temperature near the center of the core. Although coupling was improved by heat conduction through the argon gas in the chamber, the peripheral temperatures were still significantly lower than the central core temperature, resulting in a delay in the measured core deflection with respect to the average temperature.

Without heat extraction from the core and the rapid rate of core growth at elevated temperature, it was difficult to maintain steady state operation at the desired 10 kW, using manual iteration of the control loop. Virtual control drum positions were manually adjusted at each control loop iteration in attempt to maintain the desired power level, but the rapid increase in the core temperature ultimately required that power be allowed to decrease to avoid damage to the core due to elevated temperatures.

Fully automated iteration of the control loop, with automatic adjustments to the virtual control drum positions to reach and maintain the desired power level, will alleviate some of the difficulties experienced in the tests performed to date. To decrease core power, the theoretical control drum position was held constant at its final value of 113°. Without further positive reactivity insertion by virtual control drum motion, the negative reactivity introduced by core deflection provided a natural mechanism that shut down the reactor. Without heat removal, the core temperature continued to increase during the power down phase, resulting in further core deformation that increased the rate at which core power decreased to zero.

V. CONCLUSIONS

The experimental test program demonstrated the ability to couple non-nuclear testing of an electrically heated reactor system with nuclear calculations to better simulate the behavior of an operating nuclear reactor. The validation test series demonstrated that the deflection of a

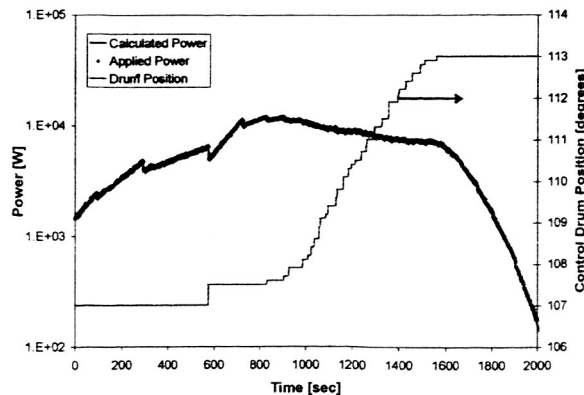


FIGURE 9. 'SAFE'-100 Power: Full Test to 10 kW, With Shut Down.

heat pipe reactor core could be reliably measured using high resolution photography.⁵ Application of this technique to provide real-time system feedback to assess the virtual neutronic response was demonstrated by a feedback control loop. Although manually iterated in the present work, the technique was successfully demonstrated. A fully automated version of the LabView control program is currently being developed.

VI. FUTURE WORK

The 'SAFE'-100 reactor core prototype is currently being removed from the vacuum chamber and is being replaced by a new test article, the 'SAFE'-100a. The 'SAFE'-100a prototype will include only the central 19 modules from the 'SAFE'-100 core geometry, but each module will include a fully operational sodium filled heat pipe and the core will be coupled to a prototypic heat exchanger. This new core configuration is expected to allow testing of the core and heat exchanger design, providing a means to simulate reactor start-up, heat pipe thaw and heat exchanger operation. The 'SAFE'-100a test article will provide conditions that more closely match an operating nuclear reactor and energy conversion system, allowing heat extraction and operation at steady state power and at isothermal conditions.

The virtual reactivity feedback control methodology will be fully automated and applied to the 'SAFE'-100a test article. Upon demonstrating successful system operation as a function of the virtual control drum position, $\theta(t)$, the control program will be modified to control reactor start-up and power transients based on the angular velocity of the control drums in order to more accurately describes the physical control in an operating nuclear reactor. Finally, a model based predictive control program will be incorporated to provide optimized reactor start-up from zero power to a pre-determined steady-state power level.¹⁴

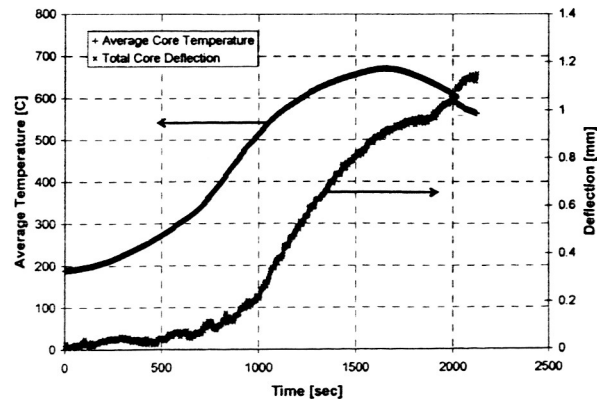


FIGURE 10. Average Core Temperature and Deflection.

ACKNOWLEDGMENTS

NASA's Project Prometheus, the Nuclear Systems Program, supported the work described within this paper, in whole or part, as part of the program's technology development and evaluation activities. Any opinions expressed are those of the author(s) and do not necessarily reflect the views of Project Prometheus. The first author was additionally supported by a NASA Graduate Student Researchers Fellowship. The author also wishes to acknowledge the substantial contributions of the EFF-TF team at NASA MSFC.

NOMENCLATURE

C	= delayed neutron concentration [neutrons/cm ²]
CTE	= coefficient of thermal expansion [mm/mm/°K]
dL	= fractional change in length [mm]
k	= effective neutron multiplication factor
L ₀	= initial core size [mm]
P	= fission power [kW]
t	= time [sec]
T	= temperature [°K]
Δ	= measured deflection from previous iteration [mm]
Δ _{set}	= set point for D for control loop iteration [mm]
λ	= delayed n precursor decay constant [sec]
Λ	= prompt n lifetime [sec]
ρ	= reactivity
θ	= angular position of control drums [degrees]

REFERENCES

1. L. OTT and R. McCulloch, "Overview of Fuel Rod Simulator Usage at ORNL," STAIF-2004, Vol. 699, p. 703-712, American Institute of Physics, Albuquerque (2004).
2. I. HRBUD, M. VanDyke, et al., "End to End Demonstrator of the Safe Affordable Fission Engine (SAFE) 30: Power Conversion and Ion Engine Operation," STAIF-2002, Vol. 608, p. 906-11, American Institute of Physics, Albuquerque (2002).
3. M. VANDYKE, "Early Flight Fission Test Facilities to Support Near-Term Space Fission Systems," STAIF-2004, Vol. 699, p. 713-719, American Institute of Physics, Albuquerque (2004).
4. M. VANDYKE, M. Houts, et al., "Test Facilities in Support of High Power Electric Propulsion Systems," STAIF-2003, Vol. 654, p. 451-456, American Institute of Physics, Albuquerque (2003).
5. M. VANDYKE, M. Houts, et al., "Phase I Space Fission Propulsion System Testing and Development Progress," STAIF-2002, Vol. 608, p. 692-7, American Institute of Physics, Albuquerque (2002).
6. L. WATERS, *MCNPX User's Manual*, Version 2.3.0, LANL, Los Alamos (2002).
7. B. STANOJEV, "Deflection Measurements of a Thermally Simulated Nuclear Core Using a High-Resolution CCD-Camera," ICAPP-2004, Paper 4278, contained within these proceedings, Pittsburgh, PA (2004).
8. M. Ash, *Nuclear Reactor Kinetics*, McGraw-Hill, Inc., New York (1965).
9. U.S. DOD, *Metallic Materials and Elements for Aerospace Vehicles*, U.S. Dept. of Defense (1998).
10. ASME, *ASME Boiler and Pressure Vessel Code, Part D: Properties*, ASME, New York (2001).
11. J. DURKEE and D. Poston, personal communication, Los Alamos, NM, January (2004).
12. D. POSTON, R. Kapernick, and R. Guffee, "Design and Analysis of the SAFE-400 Space Fission Reactor," STAIF-2002, Vol. 608, p. 578-88, American Institute of Physics, Albuquerque (2002).
13. Y. SUZUKI and Y. Arai, "Thermophysical and thermodynamic properties of actinide mononitrides and their solid solutions," *J. of Alloys and Compounds*, Vol. 271-273, p. 577-582 (1998).
14. S. BRAGG-SITTON and J.P. Holloway, "Reactor Start-Up and Control Methodologies," STAIF-2004, Vol. 699, p. 614-622, American Institute of Physics, Albuquerque (2004).